Journal of the Brazilian Society of Mechanical Sciences and Engineering (2021) 43:51
https://doi.org/10.1007/s40430-020-02721-8

TECHNICAL PAPER

Friction and wear behaviour of composite MoS_2–TiO_2 coating material in dry sliding contact

Avinash Borgaonkar[1] · **Ismail Syed**[1]

Received: 4 April 2020 / Accepted: 9 November 2020 / Published online: 4 January 2021

Abstract

Molybdenum disulphide (MoS_2) is widely used in tribological applications because of its solid lubricating properties. However, its performance needs to be further improved. In this work, an attempt has been made to improve the tribological performance of MoS_2 coating by incorporating TiO_2 nanoparticles as a reinforcement material into the MoS_2 base matrix. The effects of crystallite size and wt.% addition of TiO_2 onto the tribological properties of composite MoS_2–TiO_2 have been studied. Prior to application of the coating onto the substrate surface, it was pre-treated by phosphating which leads to improvement in the porosity and helps to enhance the bond strength between the coating and steel substrate. A tribological study of composite pure MoS_2 coating and MoS_2–TiO_2 coating was carried out using the pin-on-disc test rig at different operating conditions (contact pressure, speed and temperature). It was observed that composite MoS_2–TiO_2 coating exhibits excellent tribological properties as compared to pure MoS_2 coating. In addition, crystallite size of TiO_2 and its different weight% significantly affect the tribological properties of the composite coating. Among all samples of composite MoS_2–TiO_2 coating, the sample C (27.69 nm crystallite size) with 15% wt. of TiO_2 depicts the lowest friction coefficient and wear rate. The influence of temperature and coating thickness on the tribological properties of composite coating has been studied. The frictional coefficient has been reduced, and the wear rate increased with an increase in temperature of the coated pin surface. The similar kind of trend has been observed with respect to the coating thickness.

Keywords Coating · Composite · Molybdenum disulphide (MOS_2) · Titanium dioxide (TiO_2) · Tribological properties · Solid lubricant

1 Introduction

The interacting machine components experience friction and wear; this eventually leads to power loss and reduction in operating life. Out of the total world's power consumption, 23% is consumed by tribological contacts. Among the 23% power consumption, 20% is consumed to overcome the friction, while 3% is consumed during the replacement of the worn parts [1]. With the use of advancement in the technology such as surface modification (i.e. coating) and lubrication (usage of different oils and greases), an improved tribological response can be achieved. Eventually, this helps to reduce fuel consumption, maintenance and lifetime costs of the machine components. There are a lot of applications where the usage of liquid lubricants has limitations such as space applications (where gassing under high vacuum, high temperature circumstances occurs), food and textile industries (where contamination of the product is likely to take place), machining operations, machine components and automotive industries (where liquid lubricant is costlier) [2–4]. Nowadays most of the researchers focus on the usage of soft coating (i.e. solid lubricant) for improving the performance of the machine components having a sliding/rolling motion by reducing its friction and wear.

Since the solid lubricant has a tendency to get shear out easily, it offers better lubrication and possesses a low friction coefficient (COF). The examples of solid lubricants are soft metals (i.e. In, Pb, Sn, Ag and Au), inorganic layered compounds (i.e. MoS_2, HBN and graphite) and polymers such as Teflon [5]. The inorganic layered compound offers

Technical Editor: Izabel Fernanda Machado.

✉ Ismail Syed
syedismail7@nitw.ac.in

[1] Department of Mechanical Engineering, National Institute of Technology Warangal, Warangal, Telangana 506004, India

lower friction due to its anisotropic layered structure, i.e. covalent bonding and weak Van der Waals forces between the adjacent lamellae. For many years, molybdenum disulphide (MoS_2) has been considered as a popular solid lubricant [6], and still, many researchers are interested to determine its functionality for space applications [7–9]. Due to its lamellar structure and easy shearing ability, it provides better tribological properties at the contacting surfaces [10]. In lamellar structure, the basal plane orientation becomes parallel during the steady-state sliding motion which leads to the generation of transfer layers (002-orientation) [11]. Moreover, the parallel basal plane slides one over the other by inter- as well as intra-crystalline slip, which produces easy shear.

Generally, all solid lubricants, specifically MoS_2, have been applied using different techniques like bonding, burnishing, thin-film coating, particle embodiment and so on [12, 13]. Bonding is one of the methods used for the components and parts that are inaccessible for lubrication after assembly of the machinery. Burnishing is the simplest and economical process in which a very thin film up to 1 μm thickness can be applied by rubbing the dry lubricant powder into the surfaces requiring lubrication. In case of parts having close-fitting tolerance, thin films are applied using this process. The particle embodiment is the most commonly used method for producing a self-lubricating coated layer on metal surfaces. The thin-film coatings are produced using commercial methods such as PVD and CVD. These are costlier and used in case of an application where very fine thin films required to deposit with precision [14, 15]. From past few years, many researchers focussed on the bonded solid lubricants (BSL) since these are economical, easy to apply and having better tribological properties. Due to these advantages in the present study, BSL has been employed as a coating material.

For automotive applications, most of the engine parts which are having relative motion are made of grey cast iron. In order to investigate suitable solid lubricant, Vadiraj et al. [16] have selected four different solid lubricants like MoS_2, graphite, boric acid and TiO_2. To simulate the performance of a coating in real conditions, the experiments are carried out on pin-on-disc test rig at different load and speed conditions. From the test results, a 30–50% reduction in wear was observed in case of MoS_2 and graphite as compared remaining lubricants at all sliding velocities because of their excellent lubricity and adherence. However, boric acid indicates higher wear and COF due to the transformation of boric acid to abrasive boric oxide. In another study, Asmoro et al. [17] employed particle incorporation method to investigate the effect of solid lubricants such as MoS_2 and graphite on brake lining composite at different sliding speeds and contact pressure. Three samples of brake lining composites were prepared with the addition of various percentages of MoS_2 and graphite. The experimental findings show that MoS_2 provides better lubrication performance as compared to graphite.

The direct application of solid lubricant onto the substrate surface leads to poor adhesion. Many researchers started to employ different pre-treatment processes such as shot blasting, phosphating and salt-bath nitriding to improve the bond strength between substrate and coating [18]. As per the previously reported literature, phosphating is mostly used as a pre-treatment process as it helps to enhance the bonding between the substrate and coating by improving the porosity level [19–21]. To ensure the benefits of the phosphating process, Shankara et al. [22] fabricated a composite coating of MoS_2/ZrO_2 with different weight percentages of ZrO_2 onto the phosphated steel substrate. Their study shows that 8% of ZrO_2 in MoS_2 base matrix provides excellent tribological properties as compared to pure MoS_2. A number of studies have demonstrated that, by proper design and with the use of an advanced tribological coating such as nanocomposite and multilayer (MoS_2/Pb–Ti [23], MoS_2–Ti [24–26], MoS_2–ZnO [27], MoS_2/WSe_2 [28]), the tribological and corrosive properties can be significantly improved.

Till now, the attempts have been made to enhance the tribological properties of the bonded MoS_2 coating with different compositions of metals (MoS_2/Pb–Ti, MoS_2–Ti), selenide (MoS_2–WSe_2) and oxides (MoS_2–ZnO, MoS_2–ZrO_2). The tribological behaviour of such composites is still dramatic in nature, and meticulous examination of the contacting surfaces coated with such composite films (with different wt.% addition and crystallite size of other doping material into MoS_2 base matrix) under various operating conditions is still needed.

In the present study, a tribological analysis of developed composite coating MoS_2–TiO_2 (with in-house synthesized TiO_2 having different crystallite sizes and with different wt.% addition) was carried out on pin-on-disc test rig under different operating conditions like contact pressure, speed and temperature. The influence of coating thickness on the tribological characteristics of the composite coating is also studied. Eventually, the findings of this study will enable us to understand the effect of microstructure of coating and its composition on the tribological properties of the composite coating.

2 Materials and characterization techniques

2.1 Materials

The substrate material is AISI 52100 steel. The hardness of material is 210 HV. The steel material is prepared with dimensions 12 mm diameter and 25 mm length. Chemical composition of the substrate material is given in Table 1.

Table 1 The composition of steel material used for substrate

Fe	Cr	C	Mn	Si	Ni
96.75	1.50	1.00	0.30	0.25	0.20

The phosphating is used as a pre-treatment process on the pin surfaces to enhance the bond strength between coating and substrate. For this, the required chemicals such as phosphoric acid (H_3PO_4), magnesium carbonate ($MgCO_3$), sodium nitrate ($NaNO_2$) and sodium hydroxide (NaOH) were purchased from Sigma-Aldrich Ltd., Mumbai, India.

For depositing MoS_2 coating, the MoS_2 powder (with size 70–90 nm) was acquired from Sisco Research Laboratories Pvt. Ltd., Mumbai, India. In order to prepare the composite MoS_2–TiO_2 coating, the TiO_2 powder has been synthesized in-house. The different chemicals required for synthesizing the TiO_2 powder, such as titanium tetra isopropoxide (TTIP), acetone, methanol and sodium hydroxide (NaOH), were brought from S. D. Fine Chemicals Ltd., Mumbai, India. In order to study the effect of different crystallite sizes of TiO_2 on the tribological performance of the composite MoS_2–TiO_2 coating, the different crystallite sizes of TiO_2 powder are synthesized in-house. For the synthesis of TiO_2 nanopowder, the procedure followed which was reported by Hernandez et al. [29]. The reaction was initialised by mixing 10 mL of titanium tetraisopropoxide (TTIP) with 2 mL of acetone and 2 mL of methanol in a 300-mL beaker. This mixture was kept in an ultrasound reactor. The ultrasound reactor was initially set for 30 min which was further extended as per the requirement. A 50 mL NaOH solution was added drop-wise after the initial mixing of TTIP solution, methanol and acetone. The sonication was continued even after the complete addition of NaOH to ensure a 100% conversion of TTIP. The final product formed in the form of white precipitate was then filtered, dried and calcinated at 500-700 °C for 5 h. In order to obtain TiO_2 powder with different crystallite sizes, the same process was followed by using conventional magnetic stirrer.

In general, the binder is used to hold together the coating material on the substrate surface. In the present work, sodium silicate (Na_2SiO_3) is used as a binder to hold together the pure MoS_2 and composite MoS_2–TiO_2 coatings on the substrate surface.

2.2 Characterization techniques

2.2.1 X-ray diffraction analysis

Powder X-ray diffraction (XRD) were analysed and recorded with a Bruker D8 Advanced X-ray Diffractometer (Cu-Kα radiation, $k = 0.154056$ nm). The samples were analysed in the continuous scanning mode in the 2θ range of 20–80°, using a scan rate of 0.001° s^{-1} and used for the estimation of the crystallite size of the prepared TiO_2 powder (as per the standard Rutile, JCPDS No. 21-1276).

Table 2 Crystalline sizes of different TiO_2 samples prepared

TiO_2 sample	2θ	FWHM in radian	Average crystallite size (nm)
Sample A	25.5	0.09	90.1
Sample B	25.3	0.19	44.1
Sample C	25.2	0.31	27.7

By observing the XRD patterns, the average crystallite sizes of the synthesized TiO_2 nanoparticles were estimated using the Scherrer equation [30].

$$D = \frac{k\lambda}{\beta \cos\theta} \tag{1}$$

where D is crystallite size in nm, k is shape factor constant, which is 0.89, β is the full width at half maximum (FWHM) in radian, λ is the wavelength of the X-ray which is 1.540598 nm for Cu target $K\alpha$ radiation and θ is the Bragg's diffraction angle.

The sample A is prepared using conventional magnetic stirrer, while samples B and C using ultrasound reactor and their crystallite sizes are calculated by Scherrer equation. The sizes of synthesized nanoparticles are displayed in Table 2.

2.2.2 Surface topography

The surface topography of the pin (before pre-treatment process) and the counter face disc surface (before wear test) was measured using the Surtronic S-100 (Taylor Hobson) Series Surface Roughness Tester. To perform the surface roughness measurements, a measuring tip with a rounding radius of 2 µm was used. The required surface roughness is achieved by polishing with different grades of silicon carbide papers.

2.2.3 Scanning electron microscopy (SEM)

The morphological study of the coated specimens before and after wear tests was examined by scanning electron microscopy (SEM) in a higher-resolution field emission gun microscope, Hitachi-4800 (Tokyo, Japan), equipped with an energy-dispersive X-ray analysis (EDAX) detector (Bruker, XFlash4100, Billerica, MA, USA). The coating thickness was also measured by cross-sectioning SEM.

2.2.4 Vickers microhardness test

The microhardness of the coated samples was measured using ECONOMET VII-1 MD Microhardness tester supplied by Chennai Metco Pvt. Ltd., (Chennai, India) equipped with testing force range 10 gf to 1000 gf and automatic loading–unloading dwell period 50–60 s. The maximum resolution is 0.0625 µm.

3 Preparation and deposition of the coating

3.1 Pre-treatment process

As per the previous findings, different pre-treatment processes such as salt-bath nitriding, sand-blasting, shot peening, microarc oxidation, phosphating and abrasive blasting process were being used. Among these, more emphasis was given on the phosphating as it creates microporous which helps to trap the solid lubricant into the interstices between the phosphate crystals which results in enhanced bonding strength [31–33]. This advantage makes it a promising pretreatment, to use in this tribological study. The phosphating process was carried out as reported by Pokorny et al. [34] which involves different steps such as degreasing, pickling, rinsing, phosphating, rinsing and drying.

The substrate surface before phosphating and after phosphating is shown in Fig. 1. In Fig. 1b phosphate microporous is observed, which acts as a reservoir for solid lubricant as well as it enhances the bond strength.

The pin substrate surface before phosphating was polished with a series of different grades of polish surface such as 220, 600 and 800 grit size. After polishing the surface roughness was measured at different locations using surface roughness tester. The average surface roughness value (Ra) was observed to be 0.4 µm. Further, phosphating process was carried out on the polished specimens by the action of phosphating solution. In the similar way after phosphating the surface roughness was measured at different locations using surface roughness tester. The average surface roughness value (Ra) was observed to be 1.9 µm. The pure MoS_2 and composite MoS_2–TiO_2 coating was deposited on these phosphated samples.

3.2 Deposition of pure MoS_2 and composite (MoS_2–TiO_2) coating on substrate surface

The pure MoS_2 and composite MoS_2–TiO_2 coatings were bonded onto the substrate surface using sodium silicate (Na_2SiO_3) binder. Initially at the time of preparing the mixture, it has been observed that lesser amount of Na_2SiO_3 fails to absorb the powders, while higher amount leads to poor adhesion. After repeating a number of trials, optimum proportions of MoS_2 and Na_2SiO_3 for pure MoS_2 coating have been finalized (by wt.% 1:2.2), whereas for composite coating the wt.% of TiO_2 varied from 5 to 25% into the MoS_2 matrix and in accordance the proportion of Na_2SiO_3 were varied. The prepared coating was deposited onto the pretreated steel samples by bonding technique [22]. Finally, the coated samples were dried and cured at 150 °C for 2 h in a furnace. After deposition of the composite MoS_2–TiO_2 coating, the surface roughness of the coated surface is measured using surface roughness tester. The average surface roughness value (Ra) is observed to be 1.2 µm. Figure 2a, b shows the EDX spectrum and mapping analysis for different elements present in the pure MoS_2 and composite MoS_2–TiO_2 coating (with TiO_2 sample C and 25 wt.%). The initial spectrum (a) represents different elements which constitute for MoS_2 coatings such as Mo, S, Na, Si and O, while the other spectrum (b) shows traces of Ti along with above mentioned elements.

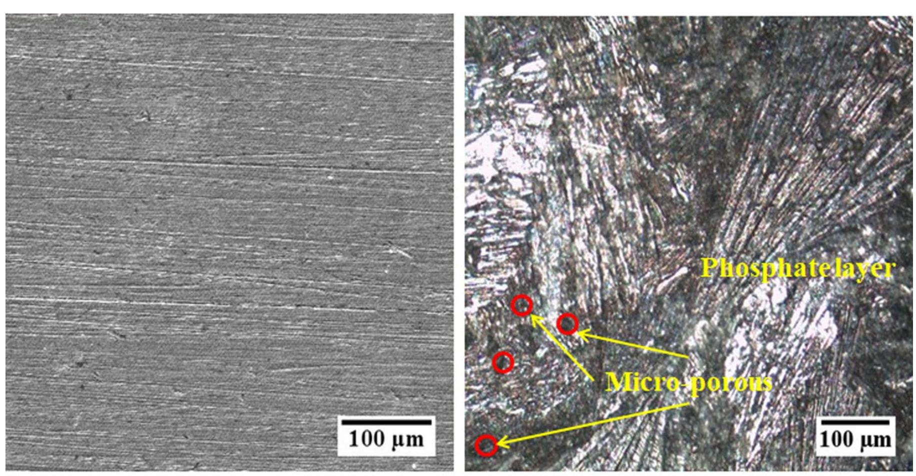

(a) (b)

Fig. 1 Substrate surface **a** before phosphating and **b** after phosphating

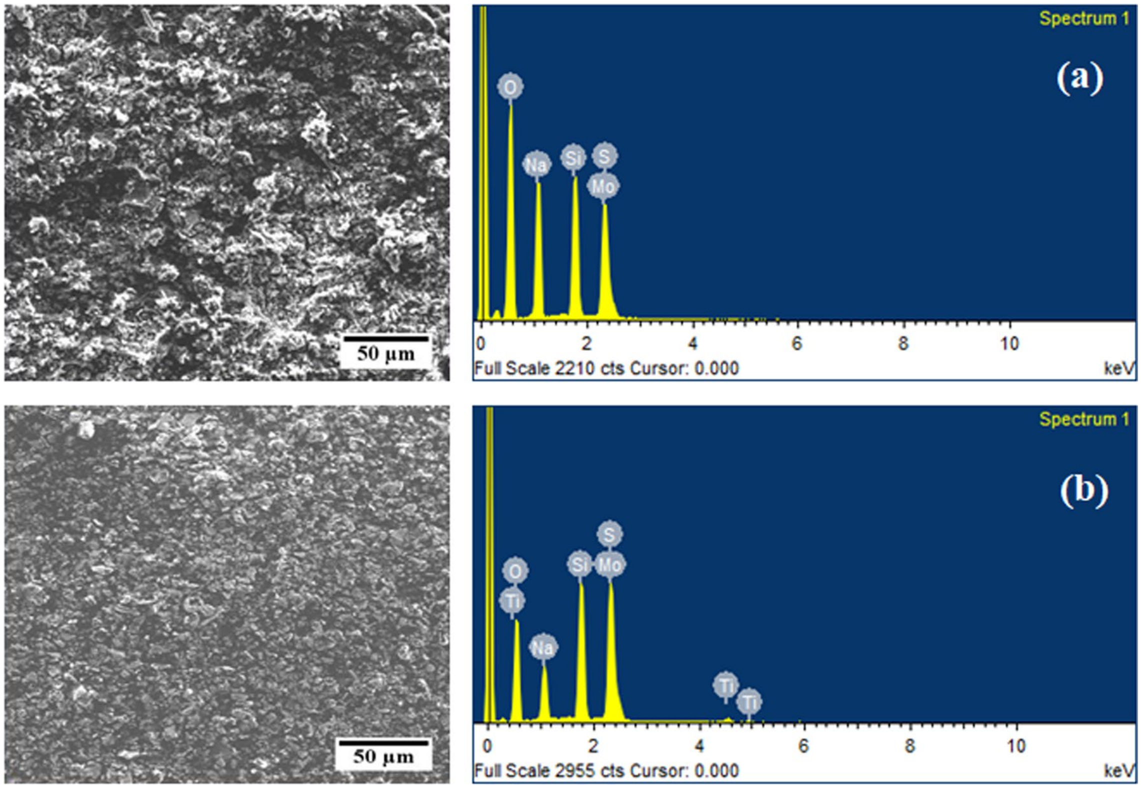

Fig. 2 EDX spectrum and mapping analysis for different elements constituted in **a** pure MoS_2 coating and **b** composite MoS_2–TiO_2 coating (25 wt.% of TiO_2 sample C)

4 Experimental analysis

The tribological study of the coated pin samples is carried out at different contact pressure, speed and temperature conditions using the pin-on-disc test rig provided by Magnum, India, referring to ASTM Standard G99-95 [35]. A schematic set-up of the pin-on-disc test rig is shown in Fig. 3. The substrate material for the pin used in this study is AISI 52100 steel. The pin is having flat end (12 mm diameter and 25 mm length), whereas the disk is made up of EN-31 steel material (165 mm diameter and thickness of 8 mm). After wear test, the pin surface is examined under an optical microscope (Model QX-4RT) which is equipped with different magnification lens (4×, 10×, 20×, 40×, 100×).

Before performing each test, the disc surface was cleaned using acetone and then dried thoroughly. The tests have been performed as per the detailed test parameters, and the operating conditions are mentioned in Table 3.

The weight loss, i.e. the difference between initial weight and final weight, is used to estimate the wear rate of the coating. In order to get the reliable data, each experiment was repeated three times. The COF and wear rate are estimated using the following equations [27].

$$\mathrm{COF} = \frac{F_\mathrm{f}}{F_\mathrm{n}} \tag{2}$$

$$\mathrm{WR} = \frac{\Delta W}{\rho \times d_\mathrm{s}} \tag{3}$$

where F_f is friction force in N, F_n is the normal load in N, ΔW is the weight loss of the coated pin in g, ρ is the density of the coated sample in g mm^{-3} and d_s is the sliding distance in m, which was calculated from sliding velocity v (m min^{-1}) and sliding time t (min).

5 Results and discussion

5.1 Effect of crystallite size and different wt.% of TiO_2 on COF and wear rate

It can be observed that the crystallite size of TiO_2 has marginal effect on the magnitude of COF and wear rate, whereas with the wt.% addition of TiO_2, contact pressure and sliding speed show a significant effect on the magnitude of COF and wear rate. The effect of crystallite size and wt.% addition of TiO_2 on COF and wear rate at different contact

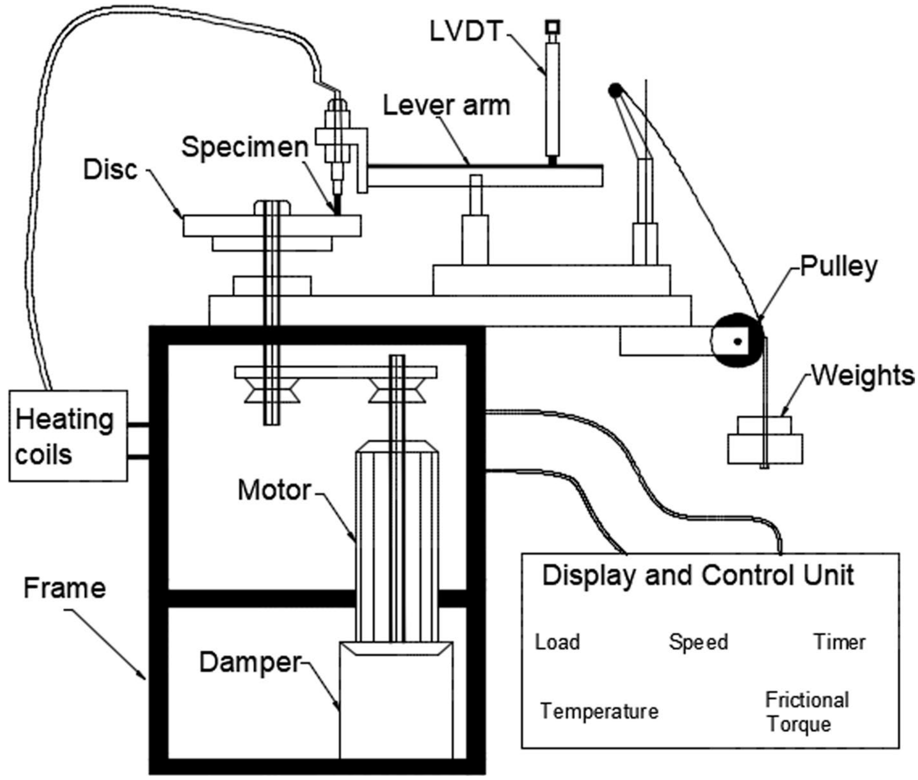

Fig. 3 Pin-on-disc tribometer schematic set-up

Table 3 Test parameters and ranges

Sr. no.	Parameters	Operating conditions
1	Contact pressure	176, 442, 707 kPa
2	Sliding speed	1, 2, 3 m s^{-1}
3	Track radius	40 mm
4	Sliding distance	3000 m
5	Temperature	RT, 100, 200, 300, 400 °C

pressures, i.e. 176 kPa, 442 kPa and 707 kPa with sliding speeds 1 m/s, 2 m/s and 3 m/s, is represented in Figs. 4, 5 and 6. The experimental results have shown that, at low contact pressure and low speed (i.e. 176 kPa and 1 m/s) composite MoS_2–TiO_2 coating (TiO_2 sample B with 15 wt.% addition) exhibits 27% reduction in COF compared with pure MoS_2 coating, whereas composite MoS_2–TiO_2 coating (TiO_2 sample C with 15 wt.% addition) demonstrates 39% improvement in wear rate compared with pure MoS_2 coating. Similarly, at high contact pressure and high speed (i.e. 707 kPa and 3 m/s) composite MoS_2–TiO_2 coating (TiO_2 sample C with 15 wt.% addition) exhibits 50% reduction in COF and 61% improvement in wear rate, respectively, as compared to pure MoS_2 coating.

The pure MoS_2 coating (denoted by 0 wt.% of TiO_2) shows higher values of wear rate and COF as compared to other samples due to poor bonding between the substrate and coating, and the coating worn out at a faster rate from the substrate (Fig. 7a). This is in line with the previous literature [22, 23] where they reported that pure MoS_2 coating possesses low wear resistance due to which it exhibits higher wear rate. The addition of TiO_2 into the base matrix of MoS_2 coating material improves the tribological properties of coated sliding contact. However, the higher concentration of doping material leads to improper mixing between the additive and base matrix which results in poor bonding due to which a reverse trend in the tribological properties was observed [26].

Figure 7 shows the pin surfaces after a tribological test carried out on pure MoS_2 and composite coating of MoS_2 with different wt.% of TiO_2 (sample C). In composite coating with the addition of TiO_2 up to 15 wt.%, the coating still remains present on the pin surfaces. The coating strongly adheres to the substrate surfaces as depicted in Fig. 7b, c which resulted in lower values of COF. As the wt.% of TiO_2 increases beyond 15%, the excess TiO_2 particles are not well mixed in MoS_2 matrix which may lead poor bonding between them. Due to this, coating worn out at a faster rate from the substrate as shown in Fig. 7d and leads to an increase in COF as well as wear rate. Furthermore, in order to understand the reason behind the increased wear rate, microhardness test was performed.

The hardness values of coated sample with synthesized TiO_2 sample C are mentioned in Table 4.

From the microhardness test, it is observed that with the increase in wt.% of TiO_2 from 5 to 25%, the hardness of

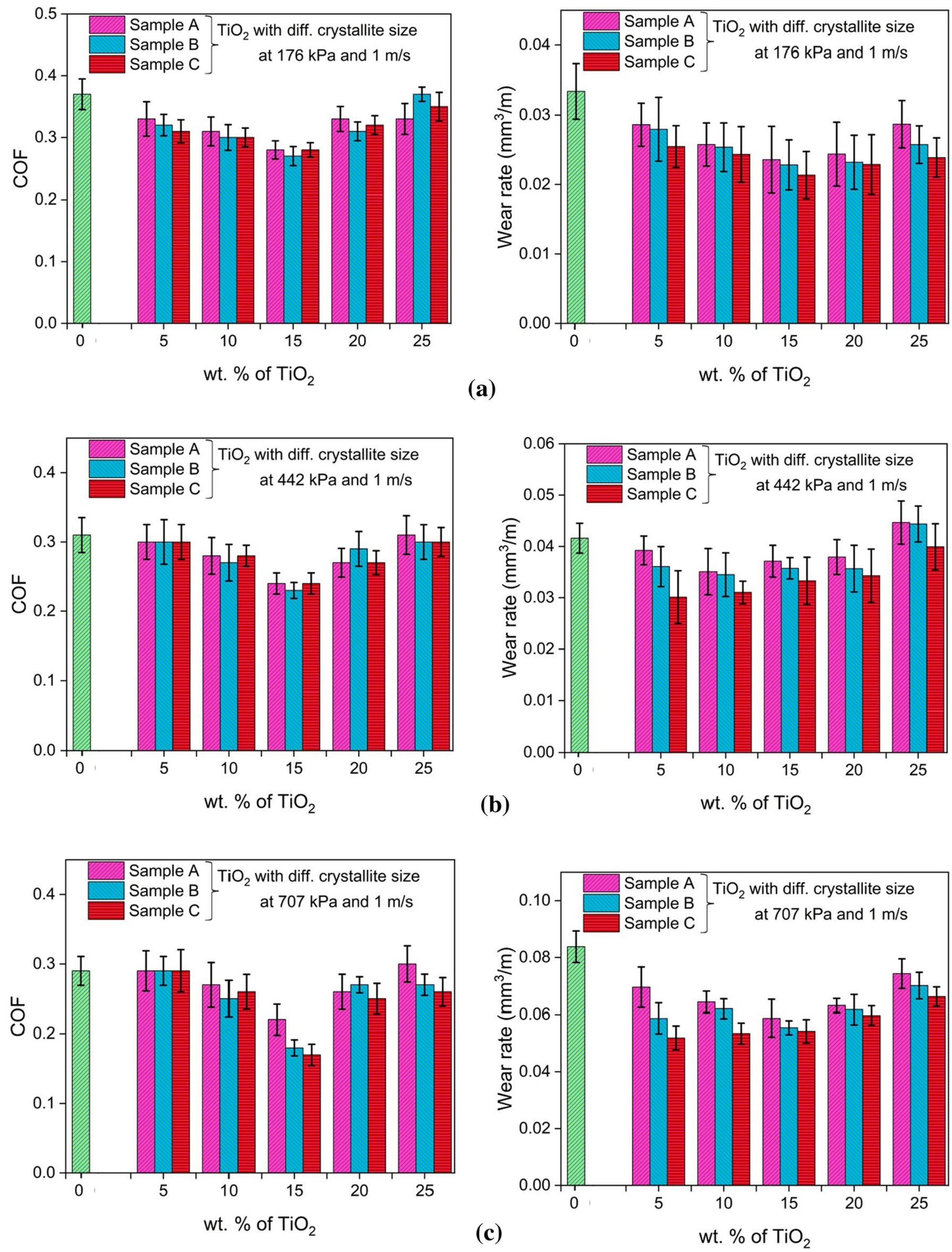

Fig. 4 Effect of addition of different wt.% of TiO_2 on COF and wear rate at **a** 176 kPa, **b** 442 kPa, **c** 707 kPa contact pressure with 1 m s^{-1} sliding speed

the coating increases. As the wt.% of TiO_2 increases, more number of particles entrapped into MoS_2 matrix which results in improved hardness [24]. This helps to improve the wear resistance. However, as the wt.% of TiO_2 increased beyond 15%, it starts deteriorating the tribological performance. Beyond 15 wt.% of TiO_2 even though the hardness

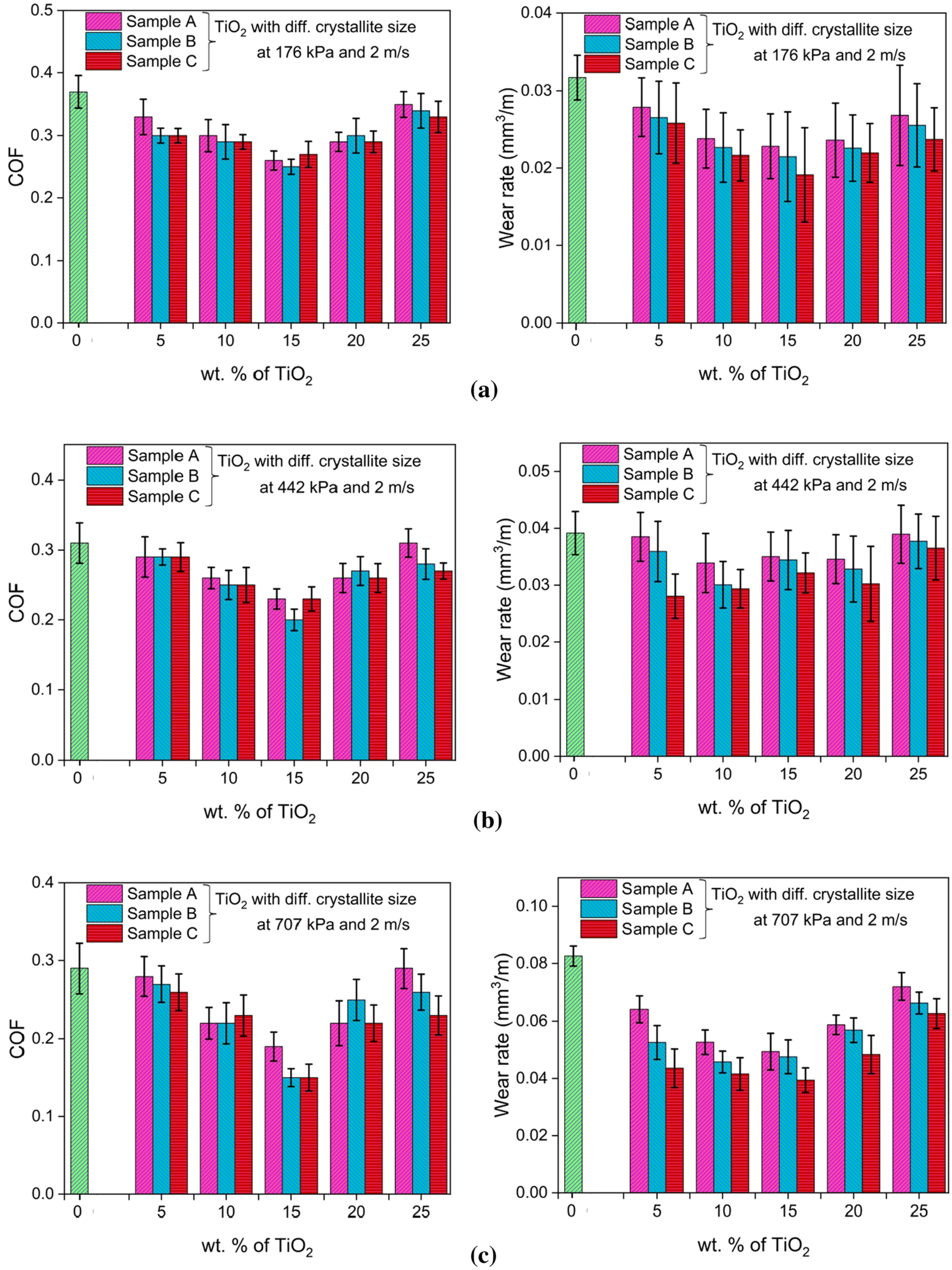

Fig. 5 Effect of addition of different wt.% of TiO_2 on COF and wear rate at **a** 176 kPa, **b** 442 kPa, **c** 707 kPa contact pressure with 2 m s^{-1} sliding speed

is increasing, at the same time the coating becomes brittle and ruptures which lead to deteriorating the performance of the coating.

As from the obtained results, composite MoS_2–TiO_2 coating developed using different wt.% of TiO_2 and crystallite size, 15 wt.% of TiO_2 with lower crystallite size 27.69 nm

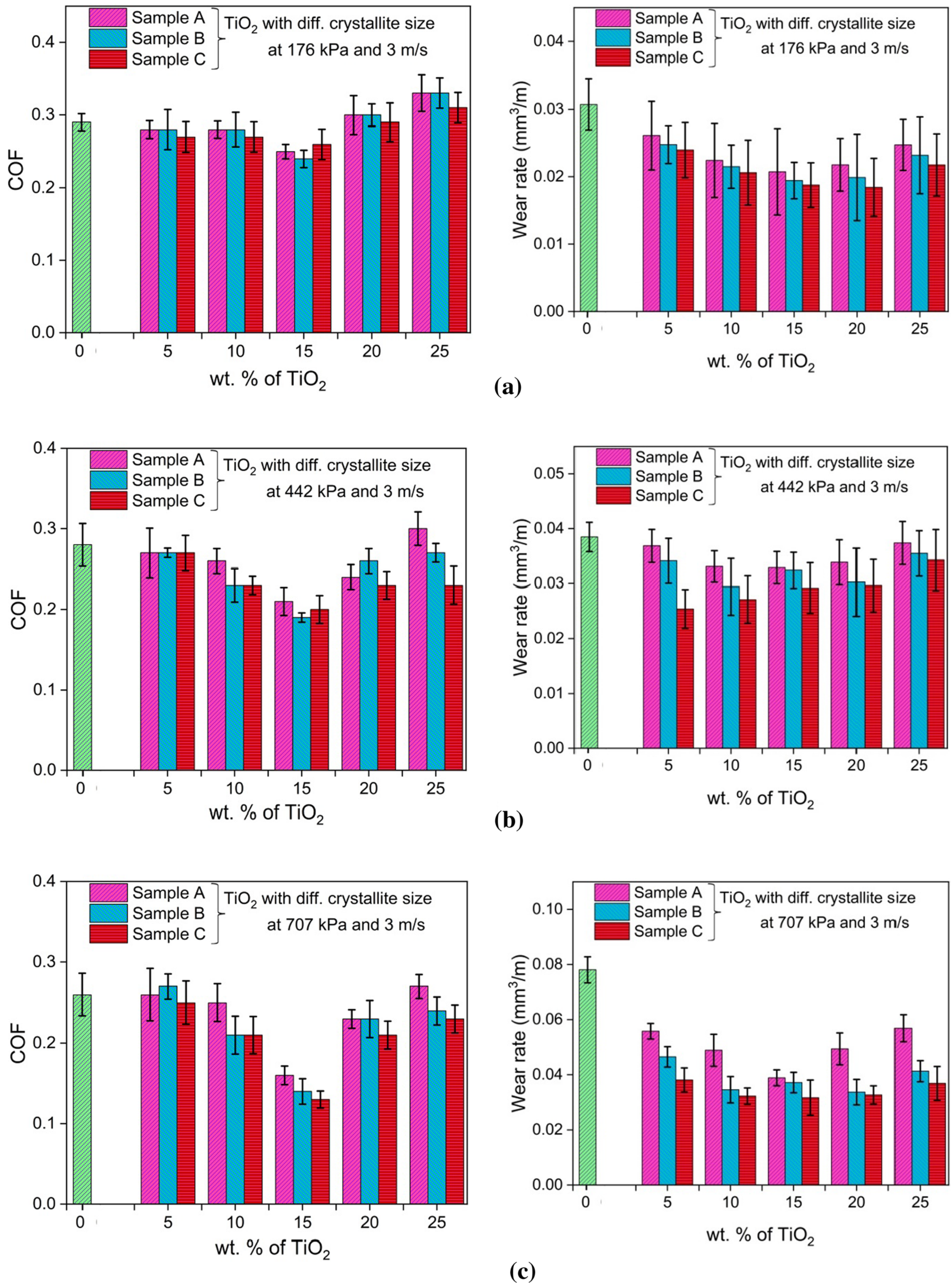

Fig. 6 Effect of addition of different wt.% of TiO_2 on COF and wear rate at **a** 176 kPa, **b** 442 kPa, **c** 707 kPa contact pressure with 3 m s^{-1} sliding speed

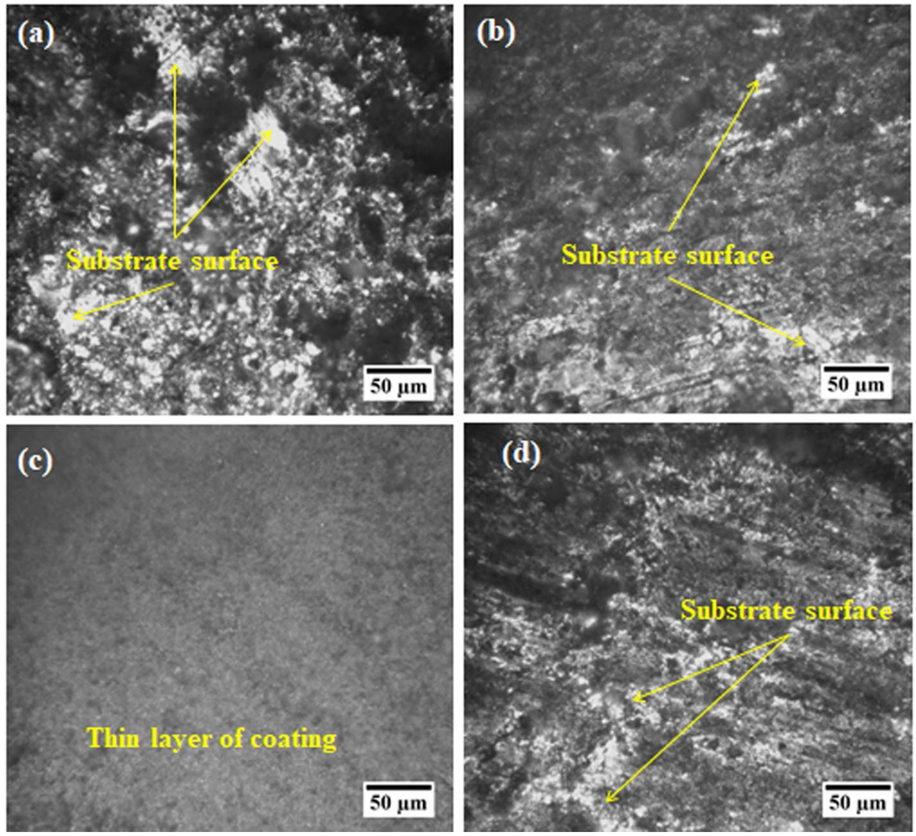

Fig. 7 Pin surface after wear test **a** pure MoS_2 and composite MoS_2–TiO_2 coating, **b** 5 wt.% of TiO_2, **c** 15 wt.% of TiO_2, **d** 25 wt.% of TiO_2 (with TiO_2 sample C)

Table 4 Microhardness values of coating comprised of different wt.% of TiO_2

Vickers microhardness in HV				
5%	10%	15%	20%	25%
19.9	27.5	31.4	36.5	49.7

(i.e. sample C) depicts the lowest COF and wear rate. Hence, for further analysis coating with this composition is taken into consideration to study the influence of temperature as well as coating thickness on the tribological characteristics.

5.2 Influence of temperature on COF and wear rate

The influence of temperature on the tribological performance of the composite MoS_2–TiO_2 coating is depicted in Fig. 8. It has been observed that COF decreases with respect to temperature and vice versa for wear rate. For other combinations of contact pressure and speed conditions, the trend followed by COF and wear rate is almost similar in nature.

The microscopic analysis of the surfaces shown in Fig. 9 depicts that when solid lubricant operated at higher temperatures, more amount of coating layer transferred from the pin surface to the counter disc surface and concentrates in the contact region. This worn-out material from the pin surface helps to form a tribolayer on to the track which enables the easy shear results in lower COF values. On the other hand, more amount of coating layer transferred to the counter disc surface results in increase in wear rate as depicted in Fig. 9. The wear rate increases with temperature could be due to oxidation, as at high temperature formation of harder MoO_3 film takes place which favours for asperity contact and removal of the coating due to ploughing [5, 36, 37]. Hence, for the composite MoS_2–TiO_2 coating from the optimum tribological performance it is better to operate up to 100 °C,

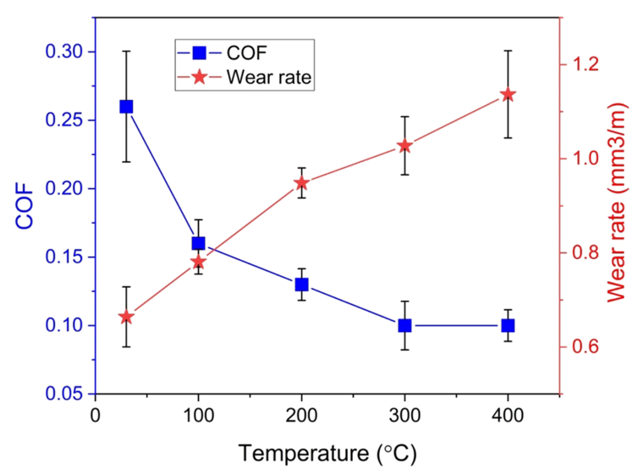

Fig. 8 Influence of temperature on COF and wear rate at 707 kPa contact pressure and 3 m s^{-1} sliding speed

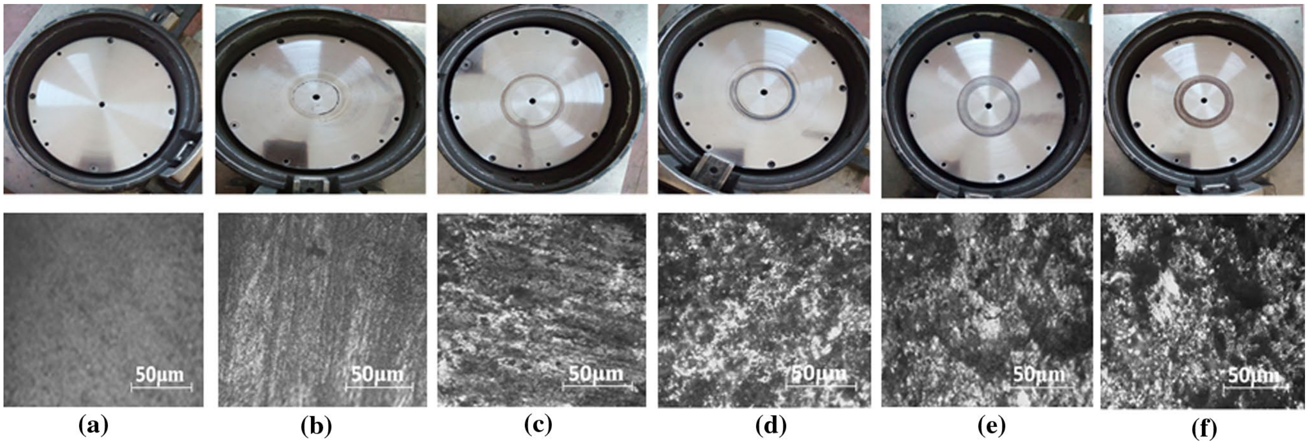

Fig. 9 Disc and pin surface **a** before test and after wear test, **b** RT, **c** 100, **d** 200, **e** 300 and **f** 400˚C at constant contact pressure 707 kPa and 3 m s^{-1} sliding speed at different temperatures

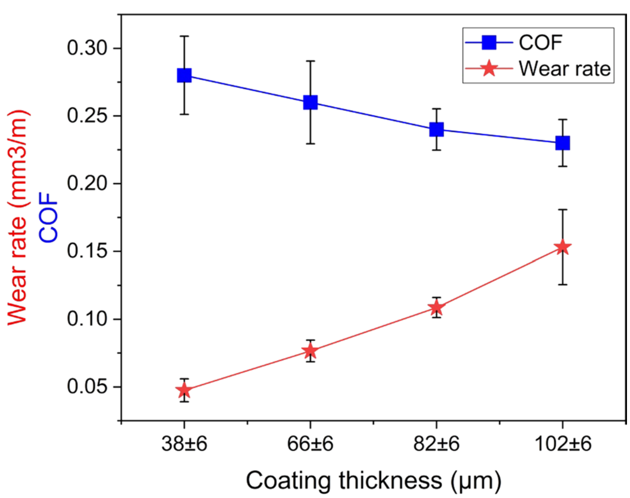

Fig. 10 Influence of coating thickness on COF and wear rate at 707 kPa contact pressure and 3 m s^{-1} sliding speed

after which in comparison with COF the wear rate increases at higher rate.

5.3 Influence of coating thickness on COF and wear rate

The effect of coating film thickness on the COF and wear rate is shown in Fig. 10. It was found that the coating film thickness has a significant effect on the tribological properties. The COF decreases with an increase in coating film thickness, whereas the wear rate increases. These findings are in line with previous studies [22, 38, 39]. The EDX analysis has been carried out to understand the behaviour of coating film thickness on the tribological properties.

Figure 11 shows the EDX spectrum and mapping analysis for different elements present in composite MoS_2–TiO_2 coating with 108 µm thickness. The EDX analysis was carried out before and after wear test for a coated sample. The initial spectrum (a) represents different elements which constitute for coatings such as Mo, S, Ti, Na, Si, O, P and C, while the other spectrum (b) shows some traces of Fe along with above-mentioned elements. The EDX analysis clearly shows that in case of higher coating thickness the coating wears out at a faster rate due to poor bonding strength. After worn-out of the coating, asperity contact between the contacting surfaces took place which can be confirmed with the traces of Fe along with the other elements.

6 Conclusion

Within the scope of this study, a successful attempt has been made for the development of composite MoS_2–TiO_2 coating material with different wt.% of TiO_2 and crystallite size. The tribological properties of the developed composite coating at different contact pressure, speed temperature and coating thickness have been investigated. The test results reveal that, in comparison with the application of pure MoS_2 coating, the composite MoS_2–TiO_2 coating exhibits excellent tribological performance in all considered operating conditions due to the synergistic effect of both MoS_2 and TiO_2. At ambient conditions, the introduction of TiO_2 into the MoS_2 matrix helps to improve the bond strength without spoiling the lubricating property of MoS_2 and in turn leads to enhancement in the endurance life of the coating. The crystallite size of TiO_2 is not influential on COF and wear rate compared to wt.% addition of TiO_2. However, at high contact pressure and higher sliding speed, the sample C (27.69 nm crystallite size) with 15% wt. of TiO_2 depicts the lowest COF and wear rate. In addition, a positive effect on COF and negative effect on wear rate are observed with

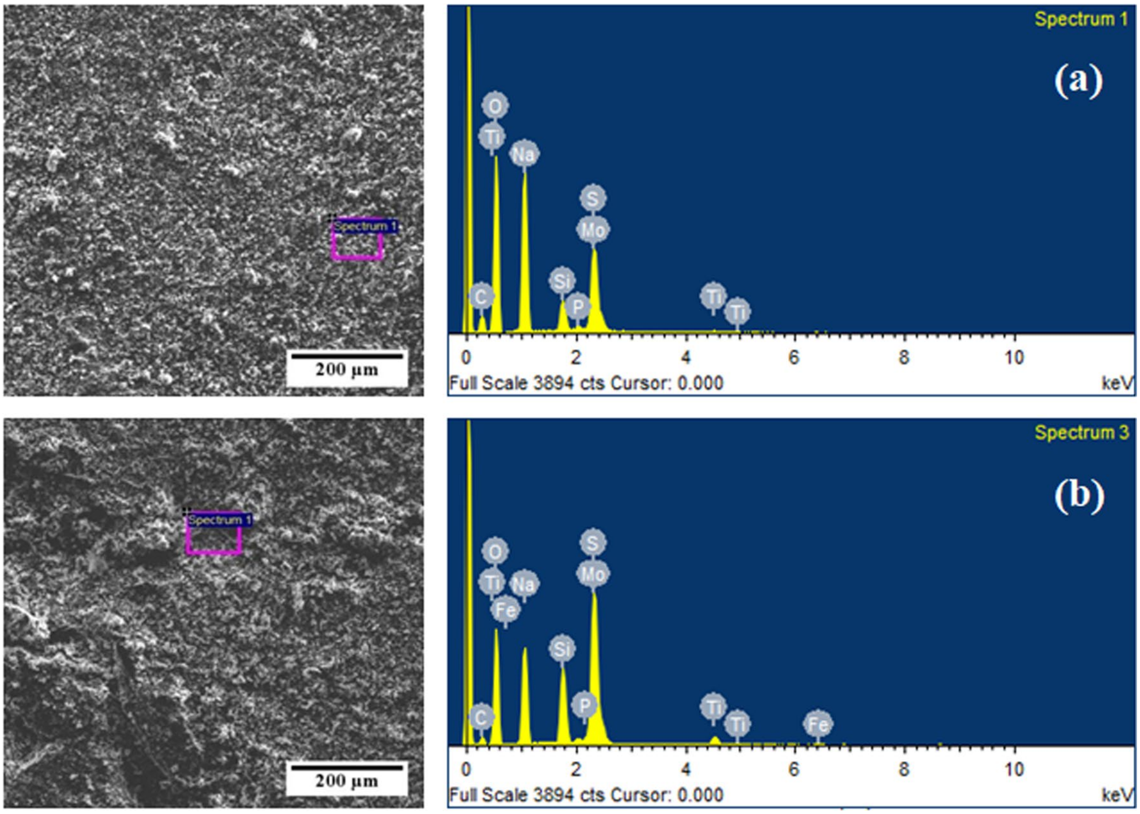

Fig. 11 EDX spectrum and mapping analysis for different elements constituted in composite MoS_2–TiO_2 coating **a** before wear test and **b** after wear test

the increase in the temperature of the coated pin surface. The similar trend is also observed with the increase in coating thickness.

Acknowledgements The authors would like to thank Dr. Shirish Sonawane, Professor, Chemical Engineering Department, National Institute of Technology Warangal, for their support in the research work. The authors would also acknowledge Center for Advanced Instrumentation, National Institute of Technology Warangal, for SEM–EDX analysis.

Compliance with ethical standards

Conflict of interest The authors declare that they have no conflict of interest.

References

1. Holmberg K, Erdemir A (2017) Influence of tribology on global energy consumption, costs and emissions. Friction 5:263–284
2. Erdemir A (2000) Solid lubricants and self-lubricating films. In: Bhushan B (ed) Modern tribology handbook. CRC Press, Boca Raton, pp 4–39
3. Liang J (2013) Bonded solid lubrication coatings, process, and applications. Encycl Tribol 1:242–247
4. Savan A, Pfluger E, Voumard P, Schroer A, Simmonds M (2000) Modern solid lubrication: recent developments and applications of MoS_2. Lubr Sci 12:185–203
5. Donnet C, Erdemir A (2004) Solid lubricant coatings: recent developments and future trends. Tribol Lett 17:389–397
6. Amaro RI, Martins RC, Seabra JO, Renevier NM, Teer DG (2005) Molybdenum disulphide/titanium low friction coating for gears application. Tribol Int 38:423–434
7. Colas G, Saulot A, Regis E, Berthier Y (2015) Investigation of crystalline and amorphous MoS_2 based coatings: towards developing new coatings for space applications. Wear 330:448–460
8. Wang P, Qiao L, Xu J, Li W, Liu W (2015) Erosion mechanism of MoS_2-based films exposed to atomic oxygen environments. ACS Appl Mater Interfaces 7:12943–12950
9. Tedstone AA, Lewis DJ, Hao R, Mao SM, Bellon P, Averback RS, Warrens CP, West KR, Howard P, Gaemers S, Dillon SJ (2015) Mechanical properties of molybdenum disulfide and the effect of doping: an in situ TEM study. ACS Appl Mater Interfaces 7:20829–20834
10. Ilie F, Tita C (2012) Modelling and experimentation of solid lubrification with powder MoS_2 through self-repairing and self-replenishing. Adv Mater Res 463:1120–1124
11. Fleischauer PD, Lince JR and Didziulis SV (2002) Chemical effects on MoS_2 lubricant transfer film formation; wear life implications. In: Handbook of tribology and lubrication, pp 30–33
12. Totten George E (2017) Solid lubricants ASM handbook. ASM International, US, pp 191–206

13. Vazirisereshk MR, Martini A, Strubbe DA, Baykara MZ (2019) Solid lubrication with MoS_2: a review. Lubricants 7:1–35
14. Hu XG, Hu SL, Zhao YS (2005) Synthesis of nanometric molybdenum disulphide particles and evaluation of friction and wear properties. Lubr Sci 17:295–308
15. Khare HS, Burris DL (2013) The effects of environmental water and oxygen on the temperature-dependent friction of sputtered molybdenum disulphide. Tribol Lett 52:485–493
16. Vadiraj A, Kamaraj M, Sreenivasan VS (2012) Effect of solid lubricants on friction and wear behaviour of alloyed gray cast iron. Sadhana 37:569–577
17. Asmoro G, Surojo E, Ariawan D, Muhayat N, Raharjo WW (2018) Role of solid lubricant (MoS_2 and graphite) variations on characteristics of brake lining composite. Mater Sci Eng 420:1–8
18. Rovani AC, Kouketsu F, da Silva CH, Pintaude G (2018) Surface characterization of three-layer organic coating applied on AISI 4130 steel. Adv Mater Sci Eng 1:1–8
19. Azhaarudeen S, Faruck AA, Nevosad A (2018) Tribological behaviour and wear mechanisms of manganese phosphate coatings under dry reciprocating sliding contact conditions. Tribol Int 122:189–199
20. Li G, Niu L, Lian J, Jiang Z (2004) A black phosphate coating for C1008 steel. Surf Coat Technol 176:215–221
21. Tamilselvi M, Kamaraj MA, Devikala S, Selvi JA (2015) Progress in zinc phosphate conversion coatings: a review. Int J Adv Chem Sci Appl 3:25–41
22. Shankara A, Menezes PL, Simha KR, Kailas SV (2008) Study of solid lubrication with MoS_2 coating in the presence of additives using reciprocating ball-on-flat scratch tester. Sadhana 33:207–220
23. Shang K, Zheng S, Ren S, Pu J, He D, Liu S (2018) Improving the tribological and corrosive properties of MoS_2-based coatings by dual-doping and multilayer construction. Appl Surf Sci 437:233–244
24. Bulbul F, Efeoglu I (2010) MoS_2–Ti composite films having (002) orientation and low Ti content. Crystallogr Rep 55:1177–1182
25. Renevier NM, Hamphire J, Fox VC, Witts J, Allen T, Teer DG (2001) Advantages of using self-lubricating, hard, wear-resistant MoS_2-based coatings. Surf Coat Technol 142:67–77
26. Ding XZ, Zeng XT, He XY, Chen Z (2010) Tribological properties of Cr-and Ti-doped MoS_2 composite coatings under different humidity atmosphere. Surf Coat Technol 205:224–231
27. Essa FA, Zhang Q, Huang X, Ali MK, Elagouz A, Abdelkareem MA (2017) Effects of ZnO and MoS_2 solid lubricants on mechanical and tribological properties of M50-steel-based composites at high temperatures: experimental and simulation study. Tribol Lett 65:1–29
28. Dominguez-Meister S, Rojas TC, Brizuela M, Sanchez-Lopez JC (2017) Solid lubricant behavior of MoS_2 and WSe_2-based nanocomposite coatings. Sci Technol Adv Mater 18:122–133
29. Hernandez-Perez I, Maubert AM, Rendon L, Santiago P, Herrera-Hernandez H, Diaz-Barriga Arceo L, Garibay Febles V, Palacios Gonzalez E, Gonzalez-Reyes L (2017) Ultrasonic synthesis: structural, optical and electrical correlation of TiO_2 nanoparticles. Int J Electrochem Sci 7:8832–8847
30. Orendorz A, Brodyanski A, Losch J, Bai LH, Chen ZH, Le YK, Ziegler C, Gnaser H (2007) Phase transformation and particle growth in nanocrystalline anatase TiO_2 films analyzed by X-ray diffraction and Raman spectroscopy. Surf Sci 601:4390–4394
31. Qiu M, Lu J, Li Y, Lv G (2016) Investigation on MoS_2 and graphite coatings and their effects on the tribological properties of the radial spherical plain bearings. Chin J Mech Eng 29:844–852
32. Duszczyk J, Siuzdak K, Klimczuk T, Strychalska-Nowak J, Zaleska-Medynska A (2018) Manganese phosphatizing coatings: the effects of preparation conditions on surface properties. Materials 11:1–22
33. Rajagopal C, Vasu KI (2000) Properties of phosphate coatings and influencing factors. In: Conversion coatings: a reference for phosphating, chromating, and anodizing processes. Tata McGraw-Hill, pp 62–70
34. Pokorny P, Tej P, Szelag P (2016) Discussion about magnesium phosphating. Metalurgija 55:507–510
35. ASTM AS. G99 (2010) Standard test method for wear testing with a pin-on-disk apparatus, pp 1–5
36. Chhowalla M, Shin HS, Eda G, Li LJ, Loh KP, Zhang H (2013) The chemistry of two-dimensional layered transition metal dichalcogenide nanosheets. Nat Chem 5:263–275
37. Borgaonkar AV, Syed I (2020) Effect of temperature on the tribological performance of MoS_2–TiO_2 coating material. In: Voruganti H, Kumar K, Krishna P, Jin X (eds) Advances in applied mechanical engineering. Lecture Notes in mechanical engineering. Springer, Singapore, pp 611–618
38. Lara LC, Costa H, de Mello JD (2015) Influence of layer thickness on sliding wear of multifunctional tribological coatings. Ind Lubr Tribol 67:460–467
39. Borgaonkar AV, Syed I (2020) Effect of coatings on rolling contact fatigue and tribological parameters of rolling/sliding contacts under dry/lubricated conditions: a review. Sadhana 45:1–16